Pergamon

Int. J. Heat Mass Transfer. Vol. 40, No. 4, pp. 773–784, 1997

0017-9310/97 $17.00+0.00

PII: S0017-9310(96)00183-4

Mixed convection flow and heat transfer between two co-rotating porous disks with wall transpiration

W. M. YAN

Department of Mechanical Engineering, Hua Fan College of Humanities and Technology, Shih Ting, Taipei, Taiwan 22305, Republic of China

and

C. Y. SOONG

Department of Aeronautical Engineering, Chung Cheng Institute of Technology, Tahsi, Taoyuan, Taiwan 33509, Republic of China

(*Received* 11 *December* 1995 *and in final form* 20 *May* 1996)

Abstract—In the present work, laminar mixed convection flow and heat transfer between two co-rotating disks with wall transpiration is investigated numerically. Both thermal boundary conditions of uniform heat flux (UHF) and uniform wall temperature (UWT) are considered. The Boussinesq approximation is invoked by taking into account the centrifugal buoyancy effects. The present paper particularly addresses the effects of wall transpiration, centrifugal buoyancy, Coriolis force, through-flow and wall-heating conditions. The numerical predictions reveal that either wall injection or wall suction has an appreciable effect on flow structure and heat transfer performance. In the case of hot-wall/cold-fluid ($Gr_\Omega > 0$), the centrifugal buoyancy has a suppression effect on the skin friction and heat transfer rates. Copyright © 1996 Elsevier Science Ltd.

INTRODUCTION

The study of flow and heat transfer between parallel porous or nonporous disks is of practical importance in the design of thrust bearings, radial diffusers, gas-turbines and compressor disks, rotating-disk contractors, etc. A vast amount of work, either theoretical or experimental, exists in the literature to study the flow and heat transfer between porous or nonporous disks. Only those relevant to the present work are briefly reviewed here. Laminar forced convection in co-rotating and stationary disk systems without wall transpiration was investigated theoretically [1, 2] and experimentally [3, 4]. The results of these investigations indicated a considerable enhancement in heat transfer for a rotating system due to Coriolis effects. Turbulent forced convection heat transfer between co-rotating nonporous disks was numerically examined by Sim and Yang [5]. It is found that disk rotation produces a surge in local Nusselt number in the near exit region and a pronounced augmentation in the average heat transfer performance. The effects of rotation-induced buoyancy on the flow and heat transfer between rotating disks without wall transpiration were studied by Chew [6], Soong [7], Soong and Yan [8, 9]. In ref. [7], a similarity analysis was employed to extensively study the influence of centrifugal buoyancy in infinite coaxial disks. Soong and Yan [8, 9] numerically examined mixed convection heat transfer between co-rotating nonporous disks with through-flow. The results in refs. [8, 9] disclosed the importance of centrifugal buoyancy effects in this class of rotating flow. Recently, with a non-isothermal through-flow in wheelspace, turbulent mixed convection flow and heat transfer was investigated by Yan and Soong [10]. They found that the centrifugal buoyancy has a considerable impact on the characteristics of flow structure and heat transfer performance.

The flow due to a rotating single disk with wall suction has been studied by Stuart [11]. His results showed that, in the presence of wall suction, the radial flow is unidirectional and decreasing; while the axial flow towards the disk wall becomes large at infinity. The effect of fluid extraction on the flow produced by a single disk was investigated theoretically and numerically by Evans [12]. Kuiken [13] presented the effect of blowing on a flow over a rotating porous disk. The results in refs. [12, 13] indicated that wall transpiration has a significant influence on the flow structure induced by a rotating disk.

Laminar forced convection between rotating porous disks was investigated by Elkouh [14]. Results for the velocity, pressure and stress were presented for various transpiration (suction or injection) rates. Flow between a stationary and a rotating disk with

NOMENCLATURE

C_f local wall skin friction coefficient, $\mu(\partial u/\partial z)_w/(\rho u_i^2/2)$
$\overline{C_f}$ mean skin friction coefficient defined in equation (8)
Gr_Ω rotational Grashof number, $(\Omega^2 s)\beta\Delta T_c s^3/\nu^2$
h heat transfer coefficient [W m^{-2} K^{-1}]
k thermal conductivity [W m^{-1} K^{-1}]
$\underline{Nu}$ local Nusselt number, hs/k
$\overline{Nu}$ mean Nusselt number defined in equation (9)
P', p' dimensionless and dimensional pressure departure, $P' = p'/(\rho u_i^2)$
Pe Peclect number, $Pr\,Re$
Pr Prandtl number, ν/α
q_w wall heat flux
R, r dimensionless and dimensional radial coordinate, $R = r/s$
R' dimensionless relative radial position, $(r-r_i)/s$
R_i dimensionless radius of opening, r_i/s
R_o downstream boundary of computational domain, r_o/s
Re through-flow Reynolds number based on inlet velocity, $u_i s/\nu$
Re_w wall Reynolds number through the porous wall, $w_w s/\nu$
Ro rotation number, $\Omega s/u_i$
s disk spacing
T temperature
T_i inlet temperature
T_w wall temperature
ΔR_1 first step size in the radial coordinate
ΔT_c characteristic temperature difference, $(q_w s/k)$ for UHF or $(T_w - T_i)$ for UWT
$\bar{U}, \bar{u}$ dimensionless and dimensional local mean velocity, $\bar{U} = \bar{u}/u_i$
U, V, W dimensionless velocity components, $(u, v, w)/u_i$
u, v, w dimensional velocity components
w_w wall transpiration velocity
Z, z dimensionless and dimensional axial coordinate, $Z = z/s$.

Greek symbols

α thermal diffusivity
β thermal expansion coefficient
θ dimensionless temperature, $(T-T_i)/\Delta T_c$
μ dynamic viscosity
ν kinematic viscosity, μ/ρ
ρ density of fluid
Ω rotational speed.

Subscripts

b bulk quantity
i inlet
o outlet
w wall condition
Ω rotation condition.

wall suction was examined numerically by Wilson and Schryer [15]. At a high Reynolds number, it was found that the equilibrium flow approaching an asymptotic state is characterized by thin boundary layers near the disk walls and an interior core rotates with nearly constant angular velocity [15]. Verma *et al.* [16] investigated steady laminar flow of an incompressible second grade fluid between two rotating porous disks. The equations of motion are solved by a regular perturbation method for small suction/injection parameters and by a quasilinearization method for strong transpiration. Recently, effects of wall transpiration on laminar convection heat transfer in rotating ducts were investigated by Soong and Hwang [17, 18] and Yan [19, 20]. Their results showed that wall suction/injection has a significant impact on the fluid flow and heat transfer characteristics.

It is noted that the study of mixed convection flow and heat transfer between rotating porous disks is useful in a practical sense but it has not received sufficient attention. In the present work, a numerical computation of the marching procedure is employed to examine the mixed convection flow and heat transfer between two co-rotating disks. The emphasis of the present work is particularly placed on the effects of wall transpiration, centrifugal buoyancy, Coriolis force, through-flow and wall-heating conditions.

ANALYSIS

Consider laminar flow through a pair of parallel circular disks rotating at an angular speed Ω, as schematically shown in Fig. 1. The annular disks of outer diameter $2r_o$ and inner diameter $2r_i$ are separated by a spacing s. The flow field is subjected to a uniform transpiration (suction or injection) of constant velocity, w_w, from the porous disk walls. The transpired fluid is same as the main flow and lies at the same temperature as the heated disk walls. The inlet coolant fluid at a uniform velocity u_i flows radially outward through the annual space between the disks. The inlet fluid is of uniform temperature T_i and the disks are symmetrically heated at a uniform wall heat flux q_w (UHF) or a uniform wall temperature T_w (UWT). A cylindrical coordinate (r, z) is fixed on the centerline with the origin at the disk center. The flow is assumed

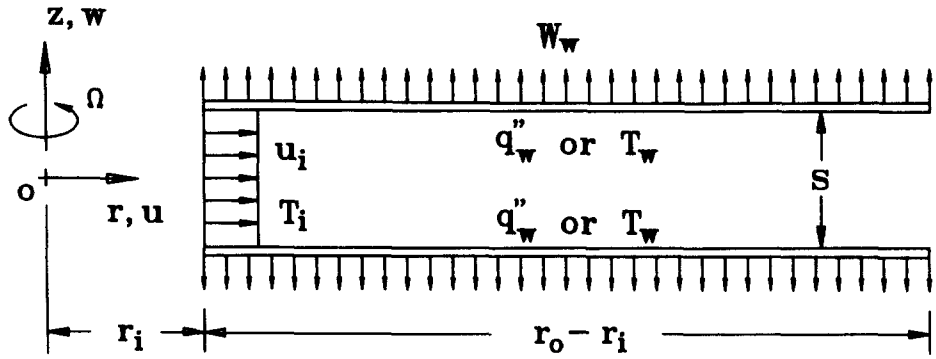

Fig. 1. Schematic diagram of the physical system.

to be steady, axisymmetric and is of constant properties except for the density variations in the centrifugal buoyancy term. Gravitational force is negligible due to its small magnitude compared to the rotation-induced centrifugal force. The Boussinesq approximation and a linear density–temperature relation, $\rho = \rho_i[1-\beta(T-T_i)]$ with ρ_i as the density evaluated at the reference temperature T_i, are invoked to take into account centrifugal buoyancy.

Governing equations

With respect to the cylindrical coordinates (R, Z) rotating with the disk system shown in Fig. 1 and introducing the following dimensionless variables and parameters,

$$R = r/s \quad Z = z/s \quad U = u/u_i \quad V = v/u_i$$

$$W = w/u_i \quad P' = p'/(\rho u_i^2)$$

$$R_i = r_i/s \quad R' = R - R_i \quad \theta = (T-T_i)/\Delta T_c$$

$$Re = u_i s/\nu \quad Re_w = w_w s/\nu$$

$$Ro = \Omega s/u_i \quad Gr_\Omega = (\Omega^2 s)\beta \Delta T_c s^3/\nu^2$$

the governing equations in dimensionless form can be formulated as [8, 9]:

$$\partial(RU)/\partial R + \partial(RW)/\partial Z = 0 \tag{2}$$

$$U\partial U/\partial R + W\partial U/\partial Z - V^2/R = -\mathrm{d}P/\mathrm{d}R + (1/Re)\partial^2 U/\partial Z^2 + 2RoV - (Gr_\Omega/Re^2)R\theta \tag{3}$$

$$U\partial V/\partial R + W\partial V/\partial Z + UV/R = (1/Re)\partial^2 V/\partial Z^2 - 2RoU \tag{4}$$

$$U\partial\theta/\partial R + W\partial\theta/\partial Z = (1/Pe)\partial^2\theta/\partial Z^2. \tag{5}$$

Due to the symmetric nature of the interested flow field, only half of the domain $R_i \leqslant R \leqslant R_o$, $0 \leqslant Z \leqslant 1/2$ is considered. The system of equations (2)–(5) is subject to the following boundary conditions:

$$R = R_i \quad U = 1 \quad V = W = \theta = 0 \tag{6a}$$

$$Z = 0 \quad \partial U/\partial Z = \partial V/\partial Z = W = \partial\theta/\partial Z = 0 \tag{6b}$$

$$Z = 1/2 \quad U = V = 0 \quad W = Re_w/Re \quad \partial\theta/\partial Z = 1(\mathrm{UHF}) \quad \text{or } \theta = 1(\mathrm{UWT}). \tag{6c}$$

An additional constraint for deduction of the radial pressure gradient in equation (3) can be derived from the global mass balance at any radial location. This constraint is expressed as:

$$\int_0^{0.5} RU\,\mathrm{d}Z = [R_i/2 - (R^2 - R_i^2)Re_w/(2Re)] \tag{7}$$

The local skin-friction coefficient $C_f = \mu(\partial u/\partial z)_w/(\rho u_i^2/2)$ and its mean value $\overline{C_f}$ can be written in dimensionless form, i.e.

$$C_f = 2(\partial U/\partial Z)_w/Re$$

$$\overline{C_f} = [2/(R_o^2 - R_i^2)]\int_{R_i}^{R_o} C_f R\,\mathrm{d}R. \tag{8}$$

Heat transfer performance is characterized by the local Nusselt number $Nu = hs/k$. The expressions for local and mean Nusselt numbers are

$$Nu = (\partial\theta/\partial Z)_w/(\theta_w - \theta_b)$$

$$\overline{Nu} = [2/(R_o^2 - R_i^2)]\int_{R_i}^{R_o} NuR\,\mathrm{d}R \tag{9}$$

where the bulk fluid temperature θ_b is defined as

$$\theta_b = \int_0^{0.5} \theta UR\,\mathrm{d}R \Big/ \int_0^{0.5} UR\,\mathrm{d}R. \tag{10}$$

Governing parameters

In this work there are two geometry parameters, R_i and R_o, and five flow/thermal parameters, Pr, Re_w, Re, Ro, and Gr_Ω. Among these, R_i is a geometry parameter directly related to the magnitude of the centrifugal effect in the entrance region. The wall Reynolds number Re_w measures the importance of the wall transpiration effect. A positive Re_w stands for the mass

Table 1. Comparisons of local Nusselt number Nu for various grid arrangements for $Re_w = -2$, $Gr_\Omega = 500$, $Ro = 0.05$, $Re = 500$ and $R_i = 20$ (UHF)

R'	I† × J‡ 201 × 201	101 × 101	101 × 51	101 × 26
2.046	6.530	6.511	6.527	6.539
5.197	4.640	4.630	4.642	4.662
10.166	3.819	3.820	3.831	3.851
15.031	3.605	3.613	3.624	3.645
20.249	3.596	3.603	3.613	3.634
30.185	3.735	3.740	3.751	3.773
40.0	3.880	3.882	3.894	3.917

† I total grid points placed in the radial direction.
‡ J total grid points placed in the axial direction.

extraction through the porous disk wall and a negative Re_w indicates the fluid injection case. The effects of the Coriolis force and the centrifugal buoyancy are characterized by rotation number Ro and rotational Grashof number Gr_Ω, respectively. It is worth noting that for radially outward through-flow, the centrifugal buoyancy has an opposing effect on the main flow. In this work, air of $Pr = 0.7$ is considered as the working fluid. In addition, the inner and outer radius of the annular disks are fixed as $R_i = 20$ and $R_o = 60$ in the computations. The ranges of the other parameters in the present study are: wall Reynolds number $Re_w = 4 - -4$, through-flow Reynolds number $Re = 250, 500, 750$ and 1000, rotational Grashof number $Gr_\Omega = 0$–10^3 and rotation number $Ro = 0$–0.1.

NUMERICAL PROCEDURE

Because the flow equations under consideration are of parabolic nature, equations (2)–(5) with boundary conditions (6) are solved using a typical marching procedure in the R-direction. The marching calculation terminates as R' reaches 40.0 or flow-reversal occurs in the flow field. In this work, a fully implicit numerical scheme with upwind difference for radial convection and central difference for axial convection and diffusion terms is employed to discretize the governing equations. The system of the discretized equations forms a tridiagonal matrix, which can be efficiently solved by the Thomas algorithm [21]. For the drastic variations of the velocity and temperature fields near the entrance and the disk walls, a non-uniform grid system of grid lines clustered in entrance and near-wall regions is employed. The first step size $\Delta R_1/(R_o - R_i) = 3.2 \times 10^{-3}$ is used and every subsequent step size is enlarged by 2% over its previous one; i.e. $\Delta R_i = 1.02\,\Delta R_{i-1}$. To examine grid independence of the calculated results, at first a numerical experiment was performed to determine the proper grid arrangement for sufficient grid resolution. Table 1 presents the local Nusselt numbers obtained on various grids. It is noted that the deviations in the local values of Nu for the computations using either $201(R) \times 101(Z)$ or $101(R) \times 51(Z)$ are always less than 1%. Accordingly, the grid of $101(R) \times 51(Z)$ is sufficient in simulation of the present fluid flow and heat transfer problem. To validate the adequacy of the numerical solutions, the predictions were compared with the measured data [3] as well as the Navier–Stokes (N–S) computations [1] in previous studies of co-rotating nonporous disks [8, 9]. It was found that the present marching solutions were in good agreement with Fig. 2 of refs. [1, 3]. These numerical tests and comparisons confirmed the accuracy and convergence of the present numerical solution.

RESULTS AND DISCUSSION

In the following presentation, firstly, consideration will be given to the solutions with uniform heat flux (UHF). Then, the results for uniform wall temperature (UWT) will be presented for exploring thermal boundary condition effects.

Uniform heat flux (UHF)

The radial developments of $U/\bar{U}$ profiles are presented in Fig. 2. For comparison, both the results for wall suction and injection are included in Fig. 2. An overall inspection of this figure shows that the developing radial velocity $U/U[fAMA]$ near the centerline is accelerated in the inlet region due to the entrance effect. As the flow goes downstream, the $U/\bar{U}$ profiles near the centerline may increase or decrease with R' due to the wall injection or suction effect. Comparison of Fig 2(a) and (b) reveals that the centrifugal buoyancy effect alters the $U/U[fAMA]$ profiles through the variation of the governing parameter Gr_Ω. In the cases of hot-wall/cold-fluid ($Gr\Omega > 0$), the centrifugal force tends to drive the dense (cold) fluid near the centerline ($Z = 0$) radially outward, i.e. buoyancy presents an accelerating or assisting effect to the main flow. On the contrary, the hot fluid adjacent to the disk wall ($Z = 0.5$) is retarded by the buoyancy-opposing effect for the global continuity. The effect of Coriolis force on the developing $U/\bar{U}$ profiles may be studied by scrutinizing Figs. 2(a)–(d). With the increase of Ro from 0.025 to 0.1, the flow field changes considerably. A larger velocity gradient is noted for a system with a higher Ro. Additionally, as shown in Fig. 2(d), there appears to be a shift of the $U/U[fAMA]$ peak from the centerline toward the porous wall. It is a reflection of the Coriolis force $2RoV$, which accelerates the fluid near the disk walls and in turn shifts the peak of $U/\bar{U}$ profile.

Figure 3 presents the developing temperature profiles at different radial locations. It is interesting to note that the results for wall suction and injection develop in a similar fashion. However, a careful look at Fig. 3 suggests that, on the porous disk wall, the thermal boundary layers for the wall injection case ($Re_w = -2$) develop a little more rapidly than those for the wall suction case ($Re_w = 2$). It implies that the heat transfer performance is better for the system with a wall suction effect. Also, as the rotation number is

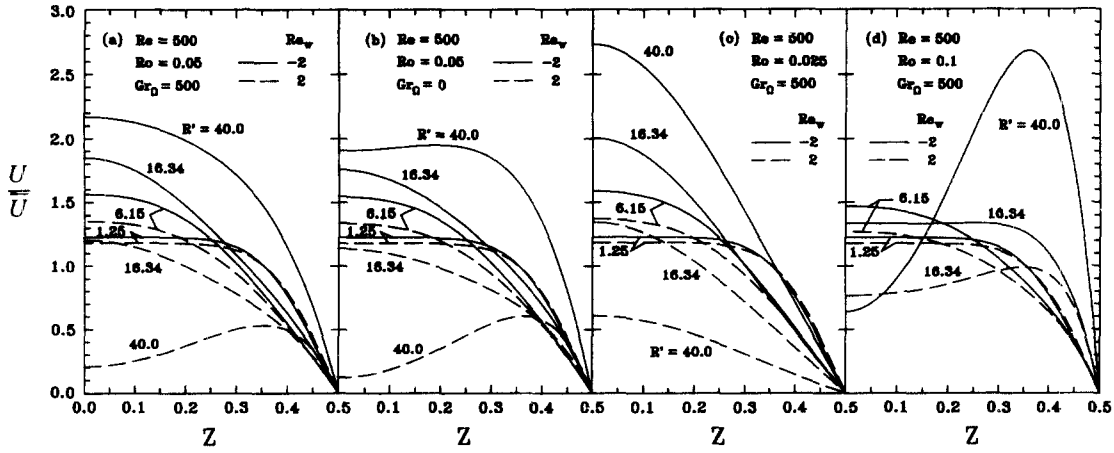

Fig. 2. Developments of radial velocity profiles (UHF).

decreased from $Ro = 0.05$ to 0.025, the development of temperature θ becomes faster and a smaller temperature gradient is found for a smaller Ro.

The effects of wall transpiration on the local friction and heat transfer performance are illustrated in Fig. 4. Relative to the result for an impermeable disk system ($Re_w = 0$), the mass extraction ($Re_w > 0$) near the entrance increases for local values of C_f. This has the effect that the wall suction attracts a large portion of the flowing mass to the near-wall region from which the fluid is extracted. The velocity gradient and thus the friction in this region increase. However, as the fluid flows in the radial direction, the mass decreases due to mass extraction, and hence the velocity gradient diminishes. This explains the reduction of the local C_f in the downstream region. For a higher suction rate, $Re_w = 4$, the mass extraction causes the occurrence of flow-reversal whose location is denoted by the symbol '×' in Fig. 4. On the other hand, the mass injection ($Re_w < 0$) has a reverse effect on the developments of the local C_f. In the downstream region, a high blowing rate ($Re_w = -4$) gives rise to a much higher C_f. In Fig. 4(b), the decrease in local Nu near the inlet is known as the 'forced-convection entrance effect'. The entrance and rotation effects (including Coriolis and centrifugal force) will eventually balance out and the local minimum Nu appears. After it reaches the minimum value, the Nu increases along the radial direction due to the rotational effect. Additionally, a larger Nu is experienced by a system with a larger suction rate

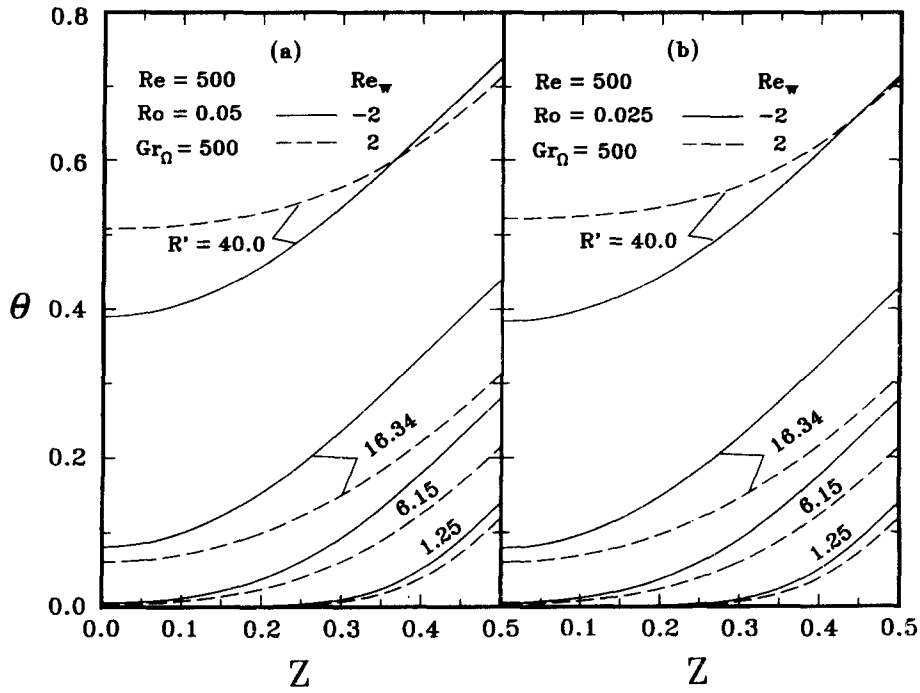

Fig. 3. Developments of radial temperature profiles (UHF).

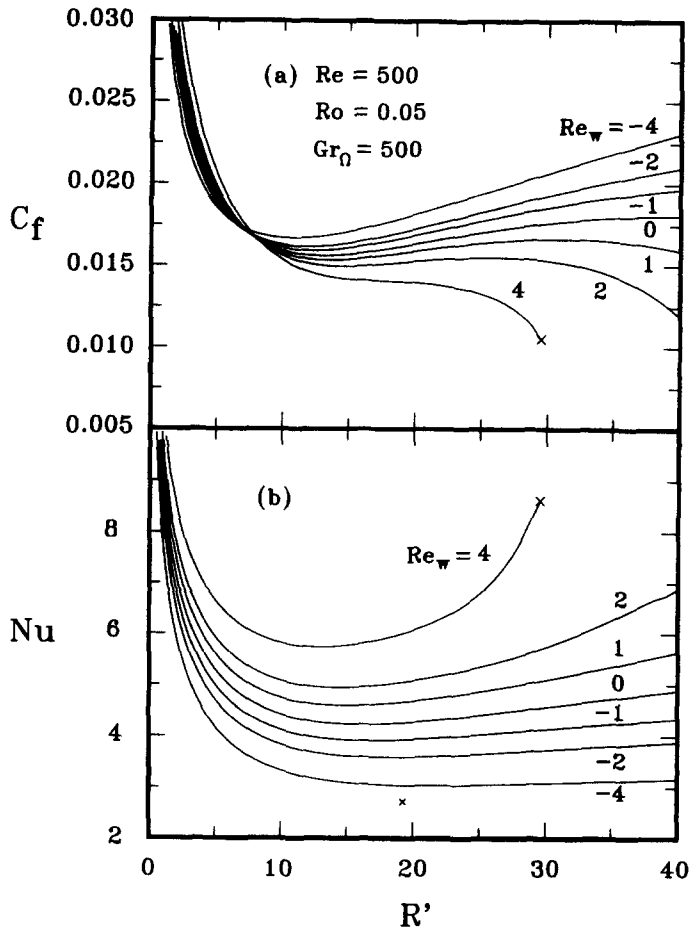

Fig. 4. Wall transpiration effects on the local C_f and Nu (UHF).

($Re_w = 4$). This is due to the fact that the difference between heated wall and bulk temperatures is smaller for a large wall suction, and hence the Nu is larger for a higher Re_w. Physically, the sucked out fluid removes a large amount of heat from the flow field.

In a disk system of high rotation rate and/or high wall heat flux, the centrifugal force plays a critical role in the flow and heat transfer characteristics. Hence, it is interesting to investigate the centrifugal buoyancy on the local C_f and Nu. Figure 5 presents the radial distribution of C_f and Nu with $Ro = 0.05$, $Re = 500$ and $Gr_\Omega = 0$, 250, 500, 750 and 1000. It is observed that the centrifugal buoyancy effect is insignificant near the entrance. In the downstream region of $R' = 5$, the centrifugal buoyancy becomes important and each curve branches out from the corresponding curve for $Gr_\Omega = 0$. Additionally, the centrifugal buoyancy diminishes the skin friction as well as the heat transfer rate, and the extent of degradation in the local C_f and Nu increases with Gr_Ω. This can be expected in a buoyancy-opposing flow, in which the centrifugal buoyancy retards the heated air flow near the porous walls and reduces the radial velocity and temperature gradients. Both the friction factor and heat transfer rates can thus be attenuated. Also, the centrifugal buoyancy has a more significant influence on the local C_f than on the local Nu. It was found from the separate numerical runs that the local centrifugal buoyancy effect diminishes as the through-flow Reynolds number Re increases.

The effects of rotation number Ro on the local C_f and Nu for $Re = 500$, $Gr_\Omega = 500$ and $Re_w = 2$ and -2 are shown in Figs. 6(a) and (b), respectively. Due to the entrance effect, as mentioned above, a monotonic decrease in local C_f and Nu near the inlet is noted. At the downstream part, say $R' > 4$, the Coriolis force becomes important and each curve branches out from the corresponding curve for the non-rotating case ($Ro = Gr_\Omega = 0$). It should be noted that the local C_f and Nu for $(Ro, Gr_\Omega) = (0.025, 500)$ are both lower than that for $Ro = Gr_\Omega = 0$; it is a consequence of the competition of the pumping effect ($Ro > 0$) and the buoyancy-opposing effect ($Gr_\Omega > 0$) in the near-wall region. Except for the curve of $Ro = 0.025$, either the local C_f or Nu increase with R' after their local minima. For $Ro > 0.025$, the pumping effect in the near-wall region becomes predominant over the buoyancy retardation; the velocity and temperature gradients can be raised with the increase of rotational rate. The local C_f and Nu, therefore, increase considerably

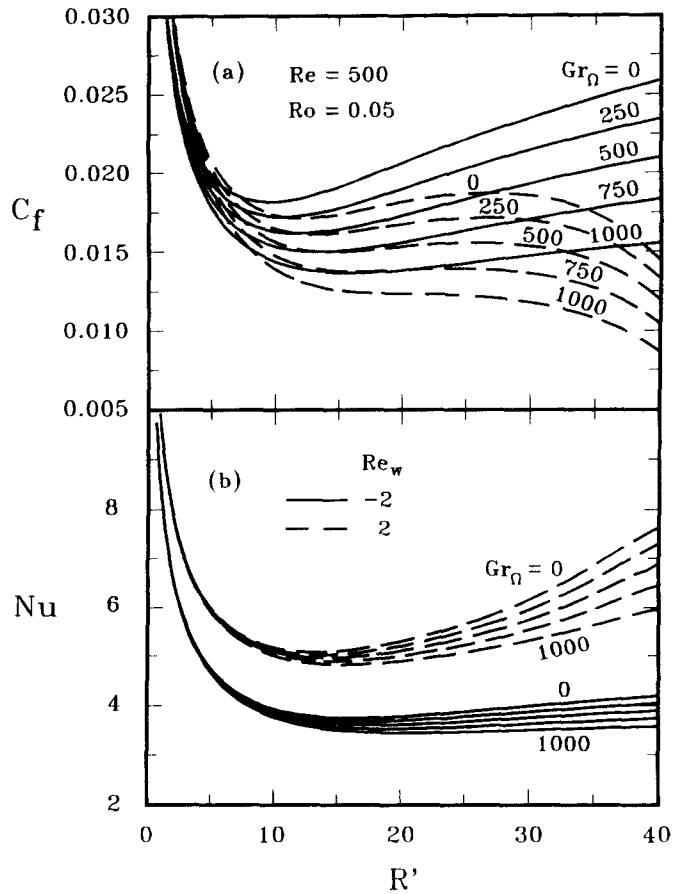

Fig. 5. Centrifugal buoyancy effects on local C_f and Nu (UHF).

throughout the rotating disks. It is also found in Fig. 6(b) that the corresponding augmentation in local Nu with the increase in Ro is more important for the wall suction case ($Re_w > 0$) than for the wall injection case ($Re_w < 0$).

Figure 7 shows the through-flow effect on the variations of local C_f and Nu for $(Ro, Gr_\Omega) = (0.05, 500)$. In Fig. 7(a), the local C_f decreases with an increase in Re. Apparently, this results from the definition of local C_f. In Fig. 7(b), on the other hand, a larger Nu is found for a system with a higher Reynolds number, Re, owing to a stronger forced-convection effect. For the case of $Re = 250$, flow reversal occurs for the relatively larger centrifugal buoyancy effect.

The effects of wall transpiration and centrifugal buoyancy on the main skin friction coefficient $\overline{C_f}$ and Nusselt number $\overline{Nu}$ are presented in Fig. 8. The present results reveal that centrifugal buoyancy attenuates both the mean $\overline{C_f}$ and $\overline{Nu}$ and the effect of Gr_Ω on the $\overline{C_f}$ is more significant than that on the $\overline{Nu}$. In addition, relative to the results for the impermeable disk system, the mass injection ($Re_w < 0$) increases the $\overline{C_f}$, while the opposite trend is observed in the case of fluid extraction ($Re_w > 0$). However, this is not the case for $\overline{Nu}$. A larger $\overline{Nu}$ is experienced for a system with a higher suction rate ($Re_w > 0$).

Uniform wall temperature (UWT)

Now attention is turned to the results of the alternative thermal boundary condition, uniform wall temperature (UWT). Shown in Fig. 9 are the radial distributions of local C_f and Nu for $Gr_\Omega = 500$, $Ro = 0.05$ and $Re = 500$ with Re_w as a parameter. A comparison of the local C_f and Nu for UHF in Fig. 4 and UWT in Fig. 9 indicates that they are similar in trend. However, close inspection of Figs. 4 and 9 discloses that, for both UHF and UWT for a system of wall fluid injection ($Re_w > 0$), a smaller C_f is noted in the region near the inlet. At a downstream (larger R') the reverse is true. Apparently, this is related to the centrifugal buoyancy effect and can be clearly found in Figs 5 and 10. A smaller Nu for all radial positions results for a system with UWT. This is consistent with the results in general conventional and forced convection duct flow; see the data in Shah and London's book [22].

Figure 10 presents the local C_f and Nu with Gr_Ω as a parameter for the UWT case. Comparing Figs 5 and 10 shows that at an upstream portion (smaller R') of the present annular passage, the local buoyancy effect is relatively stronger in the UWT case due to the higher wall–fluid temperature difference (WFTD). It is worth noting that, from equation (3), the local cen-

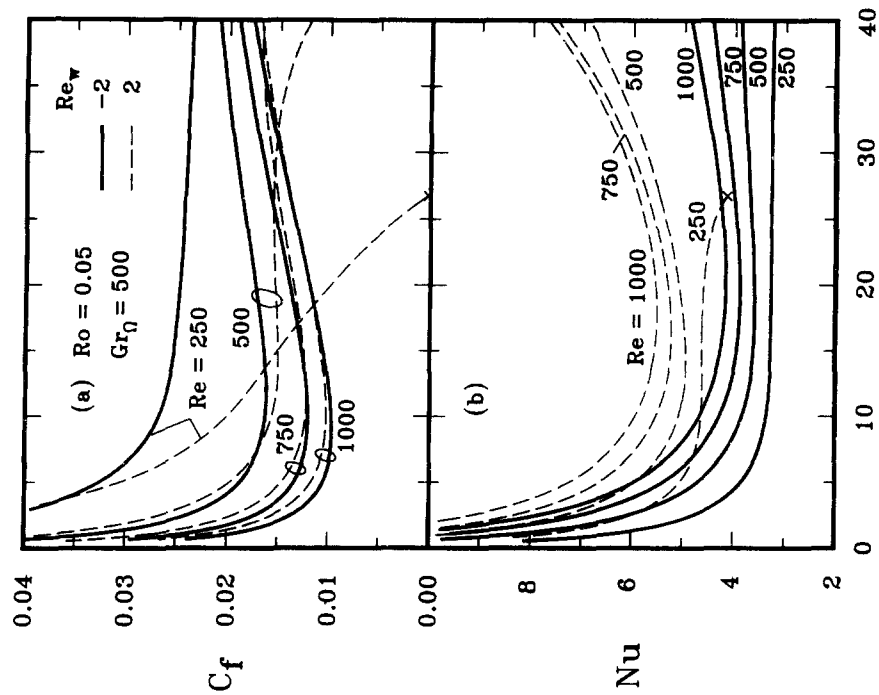

Fig. 7. Effects of through-flow Reynolds number on local C_f and Nu (UHF).

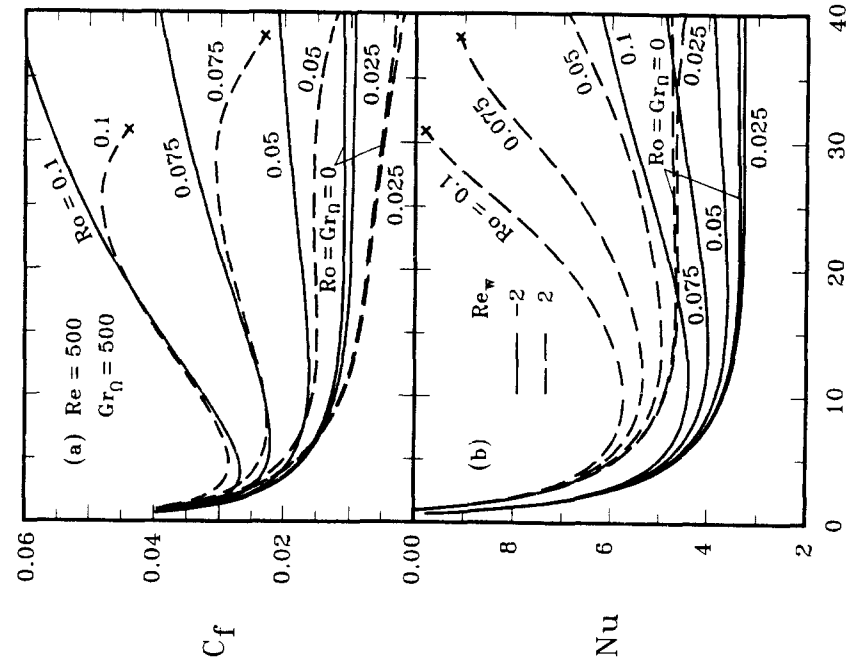

Fig. 6. Effects of rotation number Ro on local C_f and Nu (UHF).

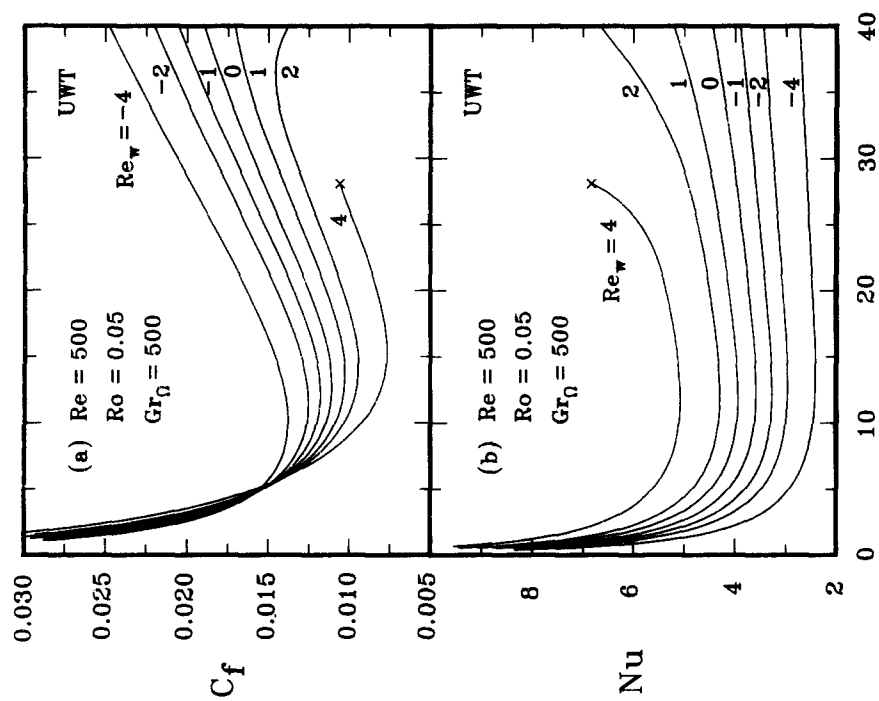

Fig. 9. Wall transpiration effects on the local C_f and Nu (UWT).

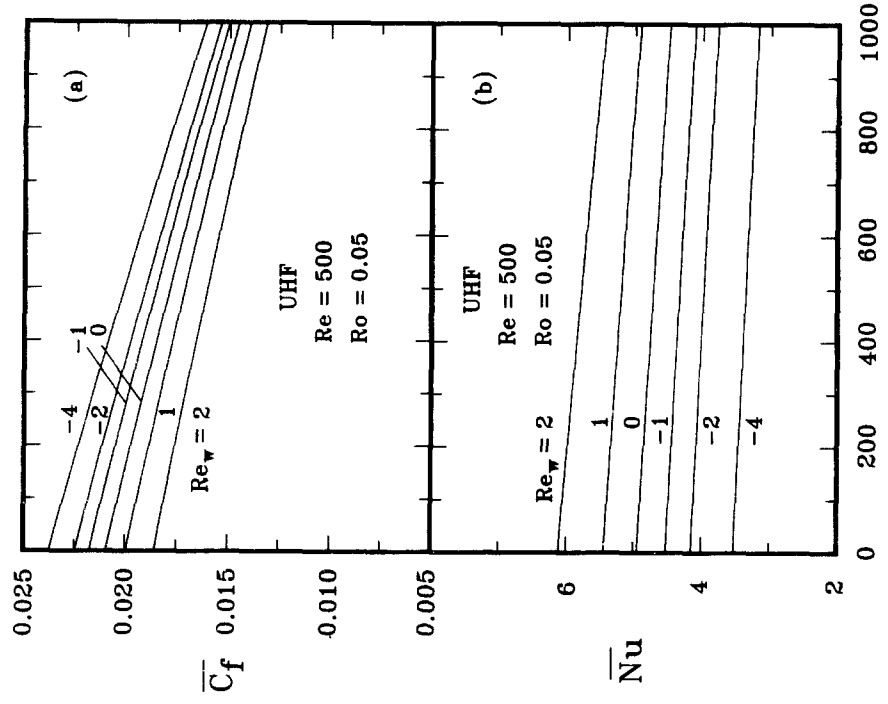

Fig. 8. Centrifugal buoyancy and wall transpiration effects on mean $\overline{C_f}$ and $\overline{Nu}$ (UHF).

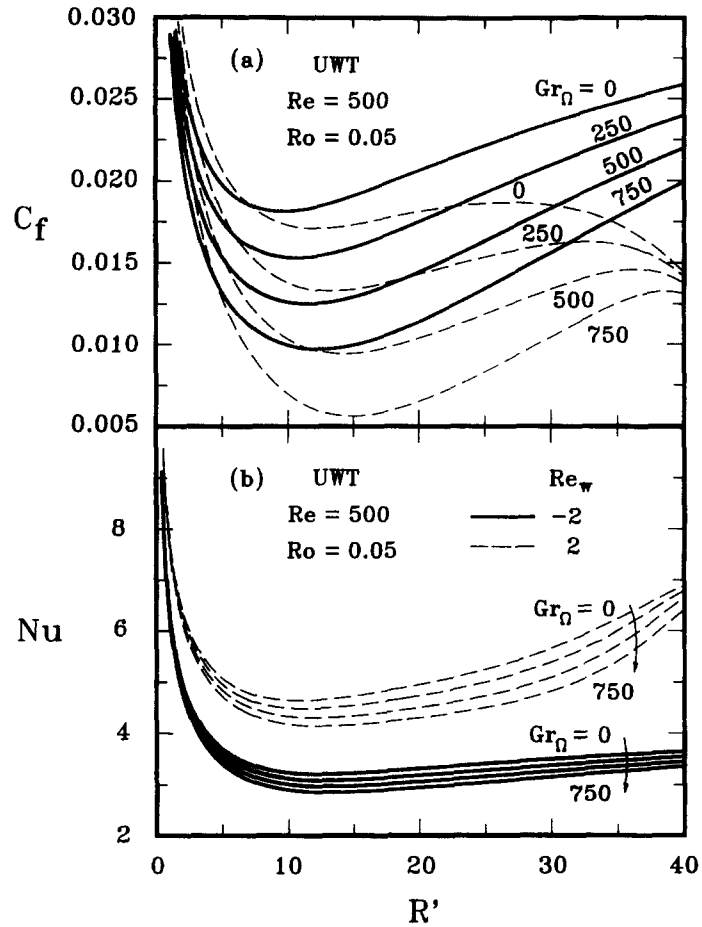

Fig. 10. Centrifugal buoyancy effects on local C_f and Nu (UWT).

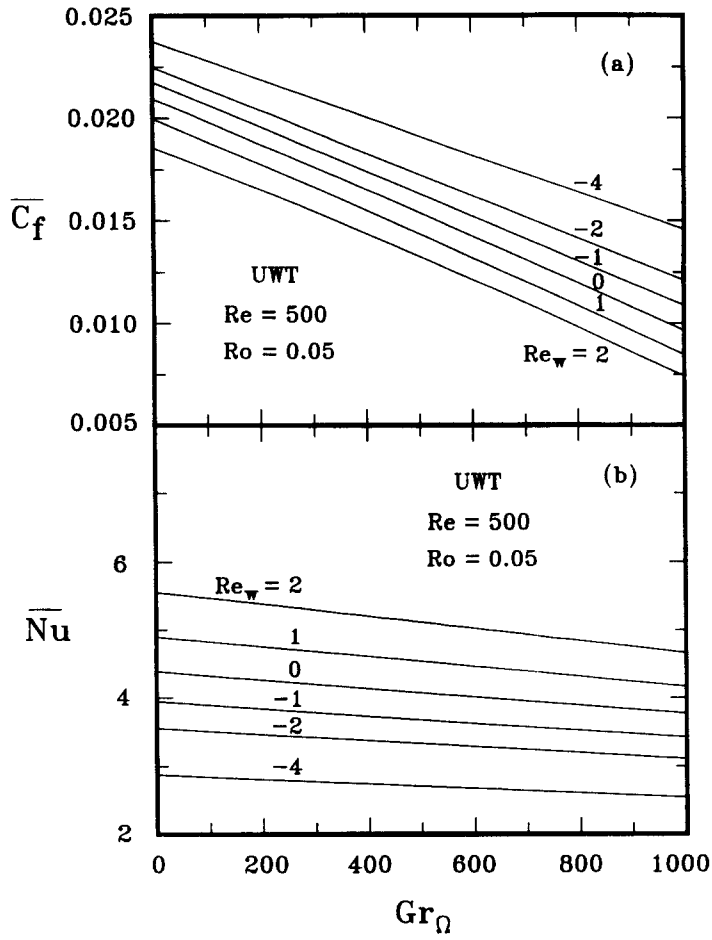

Fig. 11. Centrifugal buoyancy and wall transpiration effects on mean $\overline{C_f}$ and $\overline{Nu}$ (UWT).

trifugal buoyancy force $(Gr_\Omega/Re^2)R\theta$ depends on the mixed convection parameter $Gr\Omega/Re^2$, the radial position R and temperature $\theta(R, Z)$. With fixed Gr_Ω/Re^2 and R, the temperature distribution becomes a dominant factor for the local strength of the centrifugal buoyancy effect. As the flow goes farther downstream, WFTD approaches an invariant at the UHF condition but diminishes gradually and even approaches zero in the cases of UWT. Hence, at larger R', the local C_f and Nu for the UWT case under various Gr_Ω, respectively, approach an asymptotic curve which corresponds to the forced convection results without a buoyancy effect.

The effects of the centrifugal buoyancy and the wall transpiration on the mean $\overline{C_f}$ and $\overline{Nu}$ for UWT are illustrated in Fig. 11. Like the results for UHF in Fig. 8, the $\overline{C_f}$ and $\overline{Nu}$ decrease with increasing Gr_Ω. Also, at the same Gr_Ω, a larger $\overline{C_f}$ is noted for a system with a larger injection rate ($Re_w = -4$). But opposite effects are presented in the results of $\overline{Nu}$.

CONCLUSIONS

Numerical computations for flow and heat transfer characteristics in mixed convection between co-rotating disks with wall transpiration have been performed. The effects of wall transpiration, disk rotation, forced through-flow and wall-heating conditions on the flow and heat transfer mechanisms are investigated in detail. Based on the present results, the following summary can be drawn:

(1) The wall-suction effect enhances the heat transfer performance, while the fluid mass extraction, like the buoyancy-opposing effect, may induce flow reversal. But the wall transpiration effect on the local skin friction is complicated. Near the entrance, mass extraction ($Re_w > 0$) increases the local C_f and decreases it further downstream.

(2) The centrifugal buoyancy has a significant influence on the flow and heat transfer characteristics. Both the C_f and Nu are alleviated by the buoyancy-opposing effect, and the extent of the degradation in C_f and Nu increases with an increase in Gr_Ω.

(3) The centrifugal buoyancy has a more noticeable influence on the local skin-friction coefficient than on the local Nusselt number.

(4) For either the UHF or the UWT case, the Coriolis force can enhance both the C_f and Nu.

(5) Near the entrance, the local buoyancy effect is relatively stronger in the UWT case due to the higher WFTD. For the UWT case, however, in the downstream region, the buoyancy effect becomes small.

Acknowledgements—The financial support for this work from the National Science Council, Republic of China, under the contract NSC 82-0401-E211-016 is greatly appreciated.

REFERENCES

1. Sim, Y. S. and Yang, W. J., Numerical study on heat transfer in laminar flow through co-rotating parallel disks. *International Journal of Heat and Mass Transfer*, 1984, **27,** 1963–1970.
2. Prakash, C., Powle, U. S. and Suryanarayana, N. V., Analysis of laminar flow and heat transfer between a stationary and a rotating disk. *AIAA Journal*, 1985, **23,** 1666–1667.
3. Mochizuki, S. and Yang, W. J., Heat transfer and friction loss in laminar radial flow through rotating annular disks. *ASME Journal of Heat Transfer*, 1981, **103,** 212–217.
4. Suryanarayana, N. V., Scofield, T. and Kleiss, R. E., Heat transfer to a fluid in radial, outward flow between two co-axial stationary or corotating disks, *ASME Journal of Heat Transfer*, 1983, **105,** 519–526.
5. Sim, Y. S. and Yang, W. J., Turbulent heat transfer in corotating annular disks. *Numerical Heat Transfer*, 1985, **8,** 299–316.
6. Chew, J. W., Similarity solutions for non-isothermal flow between infinite rotating disks. Report no. TFMRC/38, Thermo-Fluid Mechanics Research Center, School of Engineering and Applied Science, University of Sussex, U.K. 1981.
7. Soong, C. Y., Theoretical analysis for mixed convection between rotating coaxial disks. *International Journal of Heat and Mass Transfer*, 1995, **39,** 1569–1583.
8. Soong, C. Y. and Yan, W. M., Numerical study of mixed convection between two co-rotating symmetrically-heated disks. *AIAA Journal of Thermophysics and Heat Transfer*, 1993, **7,** 165–170.
9. Soong, C. Y. and Yan, W. M., Transport phenomena in non-isothermal flow between co-rotating asymmetrically-heated disks. *International Journal of Heat and Mass Transfer*, 1994, **37,** 2221–2230.
10. Yan, W. M. and Soong, C. Y., Turbulent mixed convection flow and heat transfer between two co-rotating disks. *Hua Fan Annual Journal*, 1995, **3,** 213–225.
11. Stuart, J. T., On the effects of uniform suction on the steady flow due to a rotating disk, *Quarterly Journal of Mechanics and Applied Mathematics*, 1954, **7,** 446–457.
12. Evans, D. J., The rotationally symmetric flow of a viscous fluid in the presence of an infinite rotating disc with uniform suction, *Quarterly Journal of Mechanics and Applied Mathematics*, 1969, **22,** 467–485.
13. Kuiken, H. K., The effect of normal blowing on the flow near a rotating disk of infinite extent. *Journal of Fluid Mechanics*, 1971, **7,** 789–798.
14. Elkouh, A. F., Laminar flow between rotating porous disks. *Journal of Engineering and Mechanics*, 1968, **93,** 919–929.
15. Wilson, L. O. and Schryer, N. L., Flow between a stationary and a rotating disk with suction. *Journal of Fluid Mechanics*, 1978, **85,** 479–496.
16. Verma, P. D., Sharma, P. R. and Ariel, P. D., Applying quasi-linearization to the problem of steady laminar flow of a second grade fluid between two rotating porous disks. *ASME Journal of Tribology*, 1984, **106,** 448–455.
17. Soong, C. Y. and Hwang, G. J., Laminar mixed convection in a radially rotating semiporous channel. *International Journal of Heat and Mass Transfer*, 1990, **33,** 1805–1916.
18. Soong, C. Y. and Hwang, G. J., Stress work effects on similarity solutions of mixed convection in rotating channels with wall-transpiration. *International Journal of Heat and Mass Transfer*, 1993, **36,** 845–856.
19. Yan, W. M., Developing flow and heat transfer in radially rotating rectangular ducts with wall-transpiration effects. *International Journal of Heat and Mass Transfer*, 1994, **37,** 1465–1473.
20. Yan, W. M., Effects of wall transpiration on mixed convection in a radial outward flow inside rotating ducts. *International Journal of Heat and Mass Transfer*, 1995, **38,** 2333–2342.
21. Patankar, S. V., *Numerical Heat Transfer and Fluid Flow*. Hemisphere/McGraw-Hill, New York, 1980.
22. Shah, R. A. and London, A. L., *Laminar Flow Forced Convection in Ducts*, Suppl. 1 to *Advanced Heat Transfer*. Academic Press, New York, 1978.